# PROJECT UPDATE: PROTOCOL DEVELOPMENT FOR TESTING SOLDER RELIABILITY IN COMBINED ENVIRONMENTS

John McMahon[1], Polina Snugovsky[1], Jeffrey Kennedy[1], Joseph Juarez[2], Milea Kammer[2]
Ivan Straznicky[3], David Hillman[4], David Adams[4], Stephan Meschter[5],
Subramaniam Suthakaran[1], Russell Brush[1], Doug Perovic[6]

1 Celestica, 2 Honeywell, 3 Curtiss Wright, 4 Rockwell Collins
5 BAE Systems, 6 University of Toronto

**ABSTRACT**
This paper updates progress in the development of methods for investigating solder joint reliability in a combined environment of vibration and thermal cycle testing. Since combined environmental testing is an evolving concept, no default approach or standard test protocol currently exists. The need to develop such a protocol arises from the fact that materials may behave differently under combined stress conditions; exhibit different failure modes and impact the overall reliability. Combined environmental testing would therefore provide the closest approximation to actual field conditions and the best means of evaluating the performance capability of solder joints. In developing this protocol, consideration was given to obtain relevant information from both a reliability perspective (number of cycles to failure) as well as micro-structural stand point (at time of failure). Further, in combining the two conditions, time to failure had to be weighed against the overall expected time of the test; when performed alone, vibration testing is often completed within a single day, while thermal cycle testing can take up to six months to complete. Phase 1A of this project is complete and results will be presented to compare the performance of SAC305 alloy on ENIG and OSP solder pad surface coatings. Phase 1B which is in progress will involve isothermal vibration life testing over the range of alloys and temperatures. Phase 2 will then use the information to evaluate, characterize and compare various lower melt, high reliability, Bi-containing alloys against currently used SAC305 and Sn-Pb solders under combined environmental stresses.

Key words: Accelerated thermal cycling, Reliability testing, Weibull analysis

**INTRODUCTION**
This series of papers describe a proposed method for investigating solder joint reliability in a combined environment of vibration and thermal cycle testing for Sn-37Pb, SAC305, and SAC Bismuth solder alloys. In the literature review, presented in the previous paper [1], failure criteria, thermal, and vibration levels were examined to define some guidelines for the protocol. Combined protocol results will be effected by recrystallization of lead-free solder joints confounding Accelerated Thermal Cycling (ATC) results let alone adding vibration [2]. It has been reported that for ATC and vibration applied separately, sequencing is of consequence and may affect combined environments [3].

The development of a protocol for combined environment testing requires preliminary investigation over a wide range of temperatures, which will generate a wide range of failure times. It is essential to understand the relative effects of the various design variables as well as the interactions between them before we can move forward with combined environment testing. Especially if this approach is intended to evaluate alloys with identified industry potential from screening experiments [4]. The authors have established a three phase approach intended to generate relationships between the multiple sources of variation as a roadmap to a combined environment test plan. The sample sizes and alloy / surface finish combinations under study are shown in Table 1.

Phase 1A focused on isothermal Sweep and Overstress at the boundary temperatures and at important intermediate temperatures to understand the range of failure times, the relative energy required to generate failures and to confirm consistent failure modes at all temperatures.

Phase 1B which is in progress consists of isothermal testing at a constant strain range in the half power band of the resonance frequency at each of the Phase 1A temperatures. Phase 2 is currently intended to consist of combined thermal cycling and constant strain range harmonic testing over two separate temperature ranges.

**Table 1:** Test Plan

| Planned Test | Test Temp. | SAC305 | | SnPb | Violet |
|---|---|---|---|---|---|
| | | ENIG | OSP | ENIG | ENIG |
| 1A Sweep & Overstress | -55°C | 1 | 1 | | |
| | 25°C | 2 | 1 | | |
| | 75°C | 1 | 1 | | |
| | 125°C | 1 | 1 | | |
| | | | | | |
| 1B Accelerated Life Test | -55°C | 2 | | 2 | 2 |
| | 25°C | 2 | | 2 | 2 |
| | 75°C | 2 | | 2 | 2 |
| | 125°C | 2 | | 2 | 2 |
| 2 Combined | -55°C to 125°C | 3 | | 3 | 3 |
| | -40°C to 75°C | 3 | | 3 | 3 |

## EXPERIMENTAL

In this paper we will cover the isothermal Sweep and Step Stress testing of both the ENIG leg and the OSP leg completed in Phase 1A and compare lot performance over the range of temperatures.

## PHASE 1A TESTING

Phase 1A, has three primary objectives. First, it is intended to develop predictive relationships between the test temperature, the resonance frequency (RF) of the Unit Under Test (UUT), the driving G level of the table, the response G level of the UUT and the micro-strain registered at the midpoint of the span. Second, it is intended to develop a relationship between test temperature and cycles to failure in the primary technologies on the test vehicle or a similar relationship based on the work / energy absorbed by the solder joints.

Third, it is intended to compare the relative effects of ENIG and OSP surface finishes on the various parameters and isothermal step stress performance. Vibration testing is inherently more complex than accelerated thermal cycling (ATC) because the material properties of the UUT will degrade over the course of the test altering its response to the mechanical driving force. As damage accumulates the unit softens causing drift in both RF and the limits for the half power band. This damage accumulation also changes the strain range response to input G level requiring experimenters to monitor the response and adjust the input energy to maintain constant conditions over the course of the test.

This requirement for adjustment is further complicated because all of the relevant materials used in the manufacture of electronic assemblies have fundamental mechanical properties that vary with temperature. Another complexity is that failing devices cannot be removed at the time of failure. as removal will so radically change the mechanical system further testing is impossible. Therefore, investigators must choose between physical failure analyses of the structure at time of failure or continued testing to provide more failure data.

To properly define a combined environment test plan we must first understand the isothermal performance of a material set over the temperature range of interest.

The first challenge was to produce mechanically uniform material for testing. The test vehicle design provided by Honeywell and has been used extensively in mechanical testing. The units for all of Phase 1 were built together in one group using the three alloys shown in Table 1. at a Curtiss Wright facility.

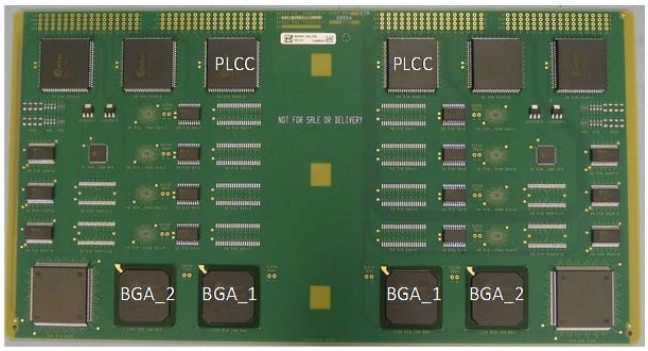


**Figure 1:** Test vehicle & tech types

Since repeatability and accuracy are critical all units were stored in a dry room and steps were taken to insure that the thermal history of all of the units varied only by the thermal requirements of the assembly alloy. To evaluate the level of variation twelve (12) serial numbers were characterized by running a sine sweep at room temperature, 1 Octave per minute and 0.4 G input acceleration between 10 Hz. And 200 Hz. before strain gauge attach. The individual results displayed in Table 2 and parametric analysis displayed in Figure 2 indicate that variation in mechanical properties are not insignificant. The mean value of the sample is 49.95 Hz. and the Standard deviation is 1.483 Hz. . Which results in a range of maximum recorded response acceleration between 7.33 G. and 13.43 G.

**Table 2:** RF & Maximum Acceleration

| M1B Sweep Summary | | | |
|---|---|---|---|
| Card Type | Card SN# | Resonant Frequency (Hz) | Max Acceleration (G's) |
| SnPb | T3000020 | 46.70 | 13.43 |
| SnPb | T3000023 | 50.94 | 10.40 |
| SnPb | T3000018 | 50.60 | 8.49 |
| SnPb | T3000014 | 48.29 | 7.33 |
| SAC | T3000039 | 50.94 | 9.14 |
| SAC | T3000047 | 48.29 | 7.93 |
| SAC | T3000048 | 49.26 | 7.57 |
| SAC | T3000052 | 50.94 | 7.71 |
| Violet | T3000065 | 50.26 | 7.67 |
| Violet | T3000068 | 50.60 | 8.59 |
| Violet | T3000070 | 50.94 | 9.06 |
| Violet | T3000073 | 51.62 | 9.16 |
| Total Cards Tested = 12 | | | |

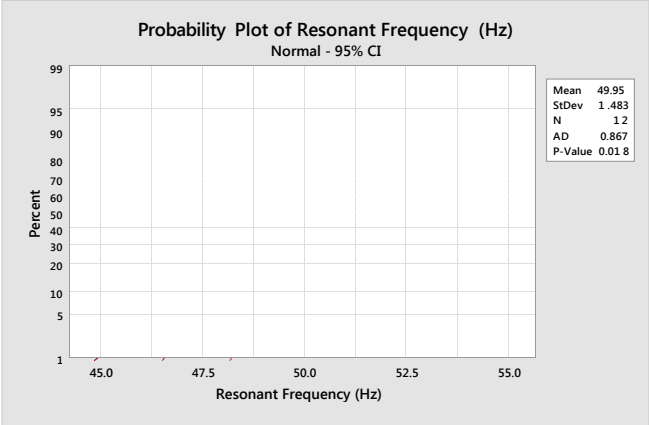


**Figure 2:** Resonance Frequency - Parametric Analysis

When combined with changes resulting from test temperature this variation can result in unexpectedly high or low strain levels at constant G levels as displayed in Table 3 [1]. The combination of a low RF and a test temperature of 75°C in SN T#-43 resulted in strain levels that deviate from the expected pattern.

**Table 3:** RF and Micro-strain

| Test Temp. | 1G ue | 2G ue | SN | RF(Hz) |
|---|---|---|---|---|
| -55 | 522.5 | 753 | T3-51 | 54.1 |
| 25 | 593 | 816 | T3-41 | 56.6 |
| 75 | 784.5 | 1046 | T3-43 | 44.3 |
| 125 | 650.5 | 908 | T3-50 | 56.3 |

This strain disparity and the resulting effect on Cycles to failure highlight the requirement going forward into phase 1B for strain controlled testing

Note that all of the results for Phase 1A testing are for SAC-305 alloy solder. Strain gauges were mounted at locations defined by the solder mask or by the vias in the footprint of the component of interest. The location of the thermocouple and the response accelerometer were also defined in the test specification. The resistance monitoring cables are hand soldered to the PTH barrels located along the free edge of the unit and all cables: resistance, strain, Thermocouples (TC) and accelerometers are strain relieved with Capton tape or flexible RTV.

**EQUIPMENT AND DATA COLLECTION**

All the equipment in utilized for this test program is summarized in Table 4. The Jaguar software system provides control for the electro-dynamic shaker table using feedback from the control accelerometer on the table and collects data from both the table and the (UUT). At 20 second intervals the system records, Time (sec), Frequency (Hz.), Control (g), Response (g), and phase angle. All of the comparative and accumulated measurements are calculated from these channels in post processing.

The two rosettes and 6 linear strain gauges attached to the UUT generate 12 micro-strain channels of data which are collected by a separate, Vishay 6000 system. Strain channels must be collected at a minimum of 500 Hz requiring that stain data is sampled at intervals to reduce the size of the data files. For the Phase 1A testing we collected strain data for the 1st, 13th and 26th minute of each step. The average positive and negative peak strain values were calculated over these one minute intervals and the range between average peak values was assigned to the test interval.

**Table 4:** Test Equipment

| Equipment | Information |
|---|---|
| Chamber | Thermotron, F-42-CHV chamber, |
| Vibration Table | Ling Dynamic Systems 8000 pound-force vertical shaker, |
| Jaguar Software | Jaguar software to operate table and record the accelerometer data |
| Strain System | Vishay System 6000 Strain system. Record strain values during first minute, 13th minute and 26th minute. Scan rate of 500Hz |
| Event Detector | STD-256 system. Cycle time 20 seconds, scan rate 2 seconds. Fail point 300 ohms. Maximum occurrence limit disabled. Software records the cycle count when a component resistance exceeds 300 ohms. |
| Temperature Monitoring | Agilent 3852A system. Monitor the ambient temperature and the board temperature every minute. |
| Fluke 73 | Hand held multimeter to verify and locate resistance failures |

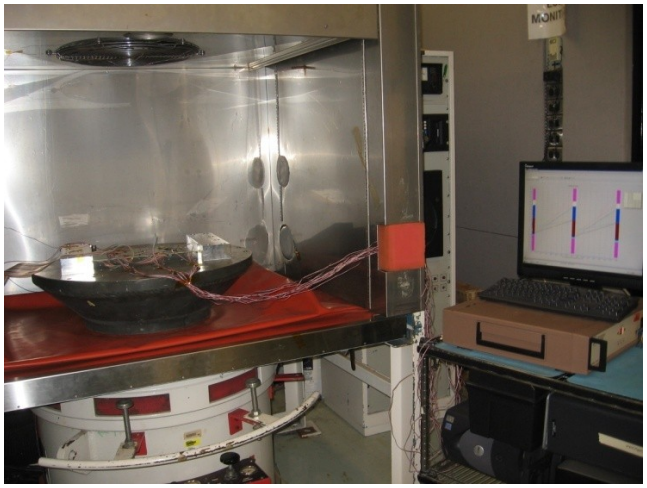

**Figure 3:** Thermal test chamber & vibration table

The ambient chamber temperature and the surface temperature of the UUT were monitored by an Agilant 3852A system which recorded data every 1 minute.

The component chains were fully in-situ monitored using an STD-256 event detector. The equipment scans all channels at two second intervals and saves data every 20 seconds. Maximum occurrence limits were disabled for this testing and the software records each cycle when the chain resistance exceeds 300 Ohms as defined in IPC9701[5]

Resistance chains that recorded 300 Ohm events during the course of a step were verified at the end of the step with a Fluke 73 multi-meter.

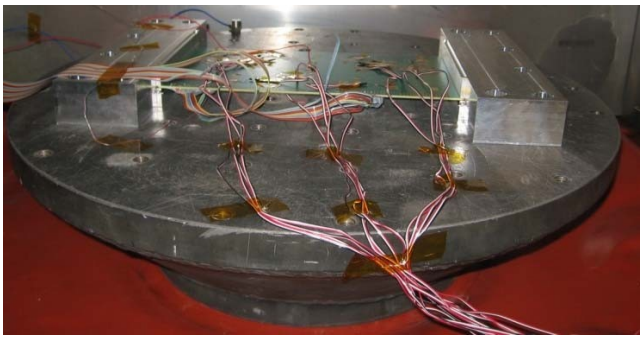

**Figure 4:** Fully instrumented UUT.

**TEST METHOD**

The step stress procedure utilized in Phase 1A incorporates multiple dwells of 100000 cycles at 1G increments until at least the four devices exposed to the highest strain levels have failed. The test is terminated at the end of the step that includes the 4th failure. The four devices are the two PLCC 84 devices and the two BGA 1156 devices closest to the centerline of bending. These devices are coded as tech types PLCC and BGA1 respectively and are labeled in Figure 1.

The detailed procedure follows: The assembled board with sensors attached was mounted on the vibration table in a custom built fixture (components down, to allow easy electrical confirmation of failed components). The cables were led outside the chamber and all connections to monitor and control systems were made and confirmed. The chamber was closed, the temperature monitor equipment engaged and the chamber was brought to test temperature and allowed to soak until the unit stabilized.

A sine sweep was performed at 1G and 4 octaves per minute between 10 Hz and 200 Hz to identify the resonance frequency and the half power band limits. These limits were then recorded by the software as control limits for the 100000 cycle dwell at 1G. This sine sweep and limit definition procedure is repeated at each subsequent step dwell.

The micro-strain collection system was started at the initiation of each dwell and records strain values at 500 Hz for 60 second periods at the defined intervals. At the termination of the dwell the vibration log file, strain log file and event detector log file were saved to record the parametric and failure data collected before initiating the next dwell. The process was repeated at increments of 1G until the primary tech type failures were recorded.

Sine sweep plots highlighting input and response G levels over the range are displayed in Figures 5 & 6. These plots display the variation in shape that can be encountered between temperatures. Compare Figure 5, SN T3-50 at 1G and 125ª to Figure 6: SN T3-51 at 1G and -55ª. The values of RF and response Gpk are different but perhaps not as significant as the differences in shape. The hot sweep exhibits a second resonance peak above 90 Hz. This peak is negligible in the cold sweep. The width of the half power band at 0.707 of the peak acceleration is also very different, producing different requirements for test control.

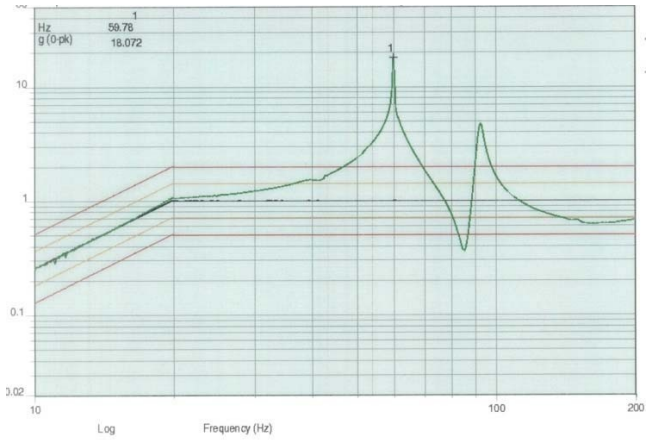


**Figure 5:** T3-50 Sine 1 Gpk 4 Oct/min at 125ª

Strain levels recorded from sine sweeps provide a view that are more readily understood by those used to manufacturing strain audits. Figure 8 displays the results from a sine sweep at 0.5Gpk input and 4 Oct/min. The pattern is typical for all of the sweeps recorded in this test phase. Resonance response can easily be 10X the response outside the half power band.

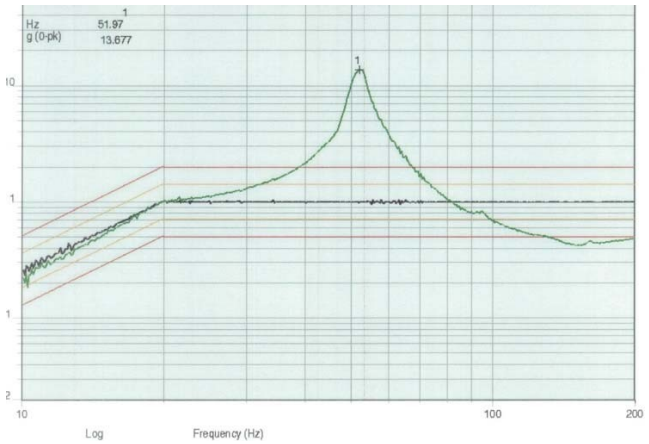


**Figure 6:** T3-51 Sine 1 Gpk 4 Oct/min at -55ª

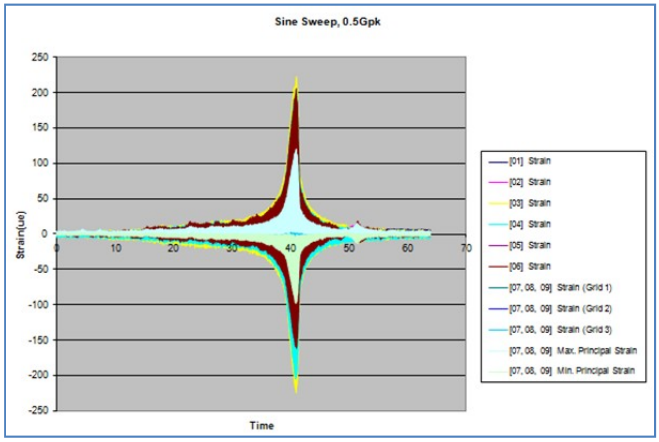


**Figure 7:** Micro-strain (ue) vs. Time (s)

**TEST RESULTS**

Each assembly has two primary failure locations for both of the technology types BGA1156 and PLCC 84. Phase 1A generated 28 failures and 2 suspensions over the four test temperatures and two surface finish lots. The Cycles to failure data is displayed in Figure 8 with vertical arrows identifying suspended data points.

Destructive analysis of BGA and PLCC devices has identified fatigue damage in the bulk solder to be the failure mode in every case. No other failure modes have been identified.

Inspection of the plotted data in Figure 8 indicates that for BGA devices the shortest life times are not at the highest temperature. This is an artifact of the low RF samples resulting in high strain levels and early failure. In previous work we reported some methods for smoothing the data and incorporating the effect of increasing strain as the step stress testing proceeds. These methods produced more ordered and expected patterns in the data graphs but were not particularly useful in predicting the ratios of cycles to failure at constant strain under isothermal testing. We have discontinued investigation into these techniques as we move into Phase 1B.

The severe impact of test temperature is evident in both Figure 8 and Figure 9 the individual cycles to failure and the main effects plot. It should also be noted that the three highest test temperatures are clearly in the creep zone for SAC305 while the -55C test temperature is more likely to resemble failure by mechanical overstress. This fact is very evident in Figure 9.

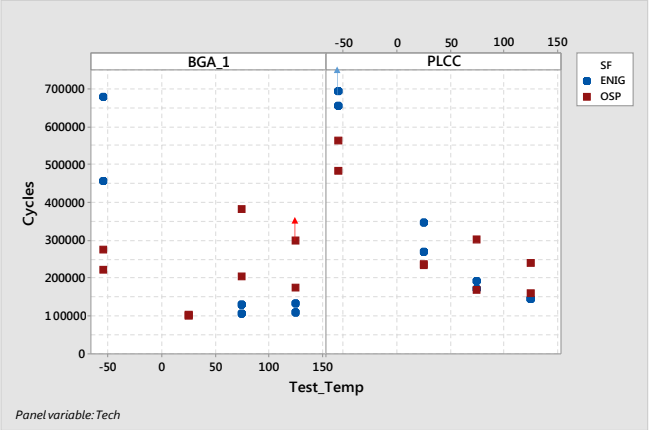


**Figure 8:** Cycles to Failure Vs. Test temperature

The plotted data also suggests that there is an interaction between surface finish and test temperature. Application of General Linear Model provides confirmation. The 4,2,2 factorial model based on Test temperature (-55, 25, 75, 125), Surface Finish (ENIG, OSP) and Tech. Type ( BGA_1, PLCC) indicates that of the primary factors only Test Temperature and Tech Type are significant at the 95% confidence level but two of the 2-way interactions are also significant. Test Temperature*Surface Finish and Test Temperature* Tech Type meet criteria for inclusion at 95% confidence. These results are apparent in the Main Effects plot and Interaction plot which are Figure 9 and Figure 10 respectively. The table of coefficients for this model is provided in Appendix A. Note that Test Temperature is modelled as a category rather than a continuous variable. This is based on differing mechanical regimes. We believe that the 25C and higher temperatures are well within the creep zone but that at -55C mechanical fatigue properties are not related to creep.

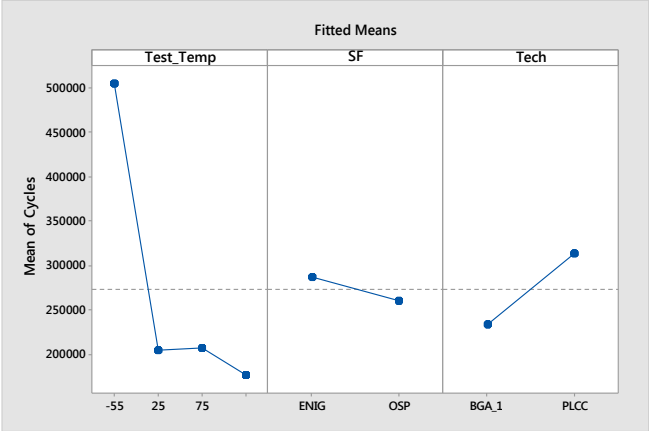


**Figure 9:** Main Effects Plot

The significance of the Test Temperature*Tech Type interaction seems reasonable based on the influence of temperature on the material properties of the package. Clearly the PWB will get harder and stronger with decreases in temperature but the BGA package substrate will harden and strengthen as well. Producing increased stress profiles in the solder. The primary driver for the PLCC is the copper lead which will not experience the same magnitude of change in properties.

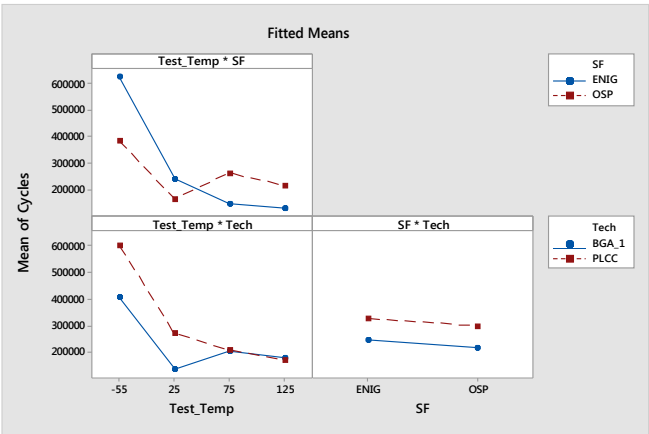


**Figure 10:** Interaction Plot

Since all of the failures are by fatigue of the bulk solder the Test temperature*Surface Finish interaction would appear to be based on the copper content of the solder joints. In all cases the SAC305 alloy has inherent copper content. In the PLCC devices the lead is always a source for Copper and the board side pad is lot dependent Ni or Cu. In the BGA

case the package side pad is plated with Ni. And the board side pad is lot dependent Ni or Cu. Based on these characteristics we expect to see more difference in the performance of the BGA devices based on Surface Finish lot because there will be a larger difference in the Cu content. This difference in the change in Cu content based on Tech Type should also be expected to contribute to the Test Temperature*Tech Type interaction.

**Table 5:** FA Samples at -55°C & 125°C

| SN | Freq. (Avg.) | Test Temp | Surface Finish | Cycles to Fail | Ref Des. | Tech | Fail / Suspend |
|---|---|---|---|---|---|---|---|
| T3000051 | 54.65 | -55 | ENIG | 4.58E+05 | U1 | BGA_1 | F |
| T3000051 | 54.65 | -55 | ENIG | 6.56E+05 | U9 | PLCC | F |
| T3000051 | 54.65 | -55 | ENIG | 6.81E+05 | U101 | BGA_1 | F |
| T3000051 | 54.65 | -55 | ENIG | 6.96E+05 | U109 | PLCC | S |
| T3000050 | 54.92 | 125 | ENIG | 1.11E+05 | U101 | BGA_1 | F |
| T3000050 | 54.92 | 125 | ENIG | 1.34E+05 | U1 | BGA_1 | F |
| T3000050 | 54.92 | 125 | ENIG | 1.44E+05 | U109 | PLCC | F |
| T3000050 | 54.92 | 125 | ENIG | 1.47E+05 | U9 | PLCC | F |
| T3000032 | 47.02 | -55 | OSP | 2.22E+05 | U101 | BGA_1 | F |
| T3000032 | 47.02 | -55 | OSP | 2.75E+05 | U1 | BGA_1 | F |
| T3000032 | 47.02 | -55 | OSP | 4.86E+05 | U109 | PLCC | F |
| T3000032 | 47.02 | -55 | OSP | 5.66E+05 | U9 | PLCC | F |
| T3000031 | 51.02 | 125 | OSP | 1.61E+05 | U9 | PLCC | F |
| T3000031 | 51.02 | 125 | OSP | 1.75E+05 | U1 | BGA_1 | F |
| T3000031 | 51.02 | 125 | OSP | 2.40E+05 | U109 | PLCC | F |
| T3000031 | 51.02 | 125 | OSP | 3.00E+05 | U101 | BGA_1 | S |

Our observations and discussions on microstructure and solder conformation are concentrated on the on the BGA devices from both surface finish lots at the extremes of test temperature. The samples under discussion are highlighted in Table 5.

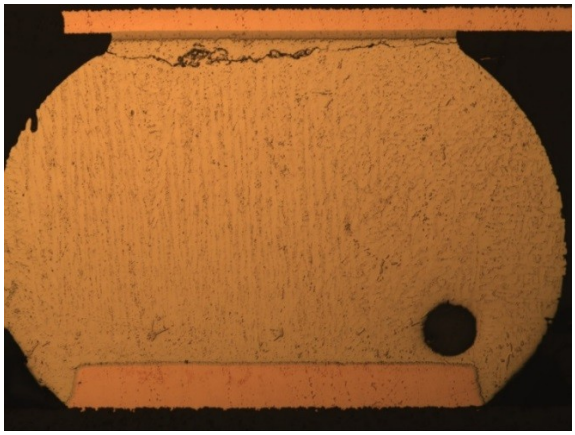

**Figure 11:** SN31 OSP 125°C 300k cycles

The solder joint in Figure 11 is from the high stress edge of U101 on SN31, an OSP board tested at 125°C and has an original magnification of 200X. The solder joint in Figure 12 is from an equivalent device and position on SN50 an ENIG board tested at 125°C. These devices have been exposed to essentially equal conditions and cycles but outcomes are significantly different.

The OSP device was suspended at 300K cycles without any 300 Ohm events, and only the displayed solder joint exhibited any damage. The net resistance had increased from 5.7 Ohms to 7.4 Ohms.

The equivalent ENIG device failed the 300 Ohm criteria at 111K cycles and every sphere on the high stress edge of the component exhibited full width cracks and significant damage by 302K cycles. Since the OSP sample had initiated a crack and resistance was rising we can assume that the difference in performance is in a range near 3 times the cycling life of the ENIG sample at 125°C.

**Figure 12:** SN50 ENIG 125°C 302K cycles.

The solder joint displayed in Figure 13 is from the high stress edge of the U1 device on SN32, it failed at 275K cycles and has been subjected to 598K cycles before this cross section was prepared.

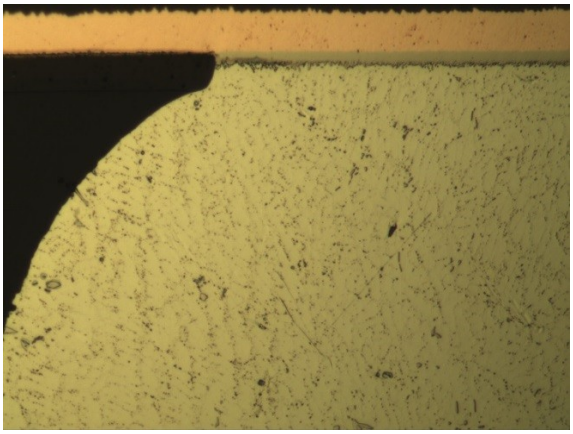

**Figure 13:** SN32 OSP -55C 598K cycles

The solder joint displayed in Figure 14 is from the high stress edge of the U1 device on SN51. It failed at 459K cycles and was cross sectioned after being exposed to 696K cycles of step stress testing. At -55C the ENIG assemblies survived on average twice as many cycles as the OSP assemblies.

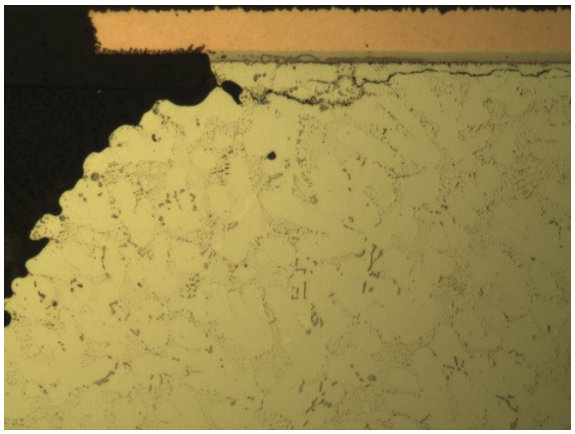

**Figure 14:** SN51 ENIG -55C 696K cycles

At resonance frequencies in the 50 Hz. Range 300K cycles requires approximately 1.7 hours of testing, even accounting for chamber ramp time there is no significant thermal aging of the microstructure in the 125°C samples. There are no significant differences between the samples tested at 125°C and -55°C for either of the surface finish lots. There are visible and consistent differences between the OSP and ENIG lots at both -55C and 125C There are visible differences in the boundary IMC layers, The spheres soldered to OSP have precipitated an additional layer of $(Cu,Ni)_6 Sn_5$ under the primary Ni IMC that exists from the ball attach process at the package assembly house. There are also noticeably more primary $Cu_6Sn_5$ particles visible in the bulk solder. As would be expected to precipitate from the higher Cu content of the molten solder during reflow. The dendritic structure of the OSP solder balls is considerably finer. βSn. Features are on the order of 7 -7.5 um in the smallest direction. Several solder spheres attached to the ENIG surface finish exhibit coarser dendrite structures on the order of 15-16 um in the smallest direction. This coarse structure also has much larger and more irregular inter-dendritic spaces. This coarser structure does not exist in every sphere, but in each cross sectional view there is a significant portion of the spheres that have this characteristic. Spheres with the fine structure can exist adjacent to a fully cracked coarse structure and exhibit very little or no damage.

There is not enough evidence to state that the difference in Cu composition is the cause of the differing performance between surface finish lots based on test temperature, but the significance of the statistical model and the striking differences in microstructure strongly suggest a correlation and seem worthy of more study.

## CONCLUSIONS

- Test procedures and data collection systems for isothermal step stress testing have been validated and refined for longer term testing.
- Step stress testing of units with resonance frequencies near 50 Hz can generate solder fatigue failure modes at a step length of 100K cycles and step increments of 1G.
- Test temperature is the dominant factor in determining expected lifetime under sine wave vibration.
- Technology Type is also a significant factor.
- Surface Finish is not a significant factor over the range of this testing but the Interaction between Surface finish and test temperature is significant, affects the basic microstructure and deserves more investigation.
- The interaction between test temperature and technology type is dependent on the geometry and mechanical properties of the various components but may also be impacted by the microstructural changes associated with device types.

## FUTURE WORK

Phase 1B, Isothermal fatigue testing using sine wave vibration inside the half power band of the Resonance frequency is underway. The project team intends to complete Phase 1B in Q4 of 2016 and proceed quickly to Phase 2.

## ACKNOWLEDGEMENTS

This work is funded by the Refined Manufacturing Acceleration Process (ReMAP) and member companies.
The authors would like to acknowledge several Celestica employees Kamran Sodaei, Parisa Najafi, Amit Prajapati and Ariana Khakpour for their contributions to the testing and failure analysis of these samples.

## REFERENCES

1. J.McMahon, J.Juarez, P.Snugovsky, J.Kennedy, M.Kammer, I.Straznicky, D.Hillman, D.Adams, S.Meschter, S.Suthakaran, R.Brush, D.Perovic, Protocol Development For Testing Solder Reliability In Combined Environments, SMTA ICSR, May 2016
2. A. Mayyas, L. Yin, P. Borgesen, “Recrystallization of Lead-free Solder Joints-Confounding the Interpretation of Accelerated Thermal Cycling Results”, Proceedings of the ASME 2009 International Mechanical Engineering Congress & Exposition, November 13-19, Lake Buena Vista, Florida, USA.
3. A. Perkins, S.K. Sitaraman, “A Study into the Sequencing of Thermal Cycling and Vibration Tests”, IEEE 2008 Electronics Components & Technology Conference.
4. J. M. Juarez, P. Snugovsky, E. Kosiba, Z. Bagheri, S. Suthakaran, M. Robinson, J. Heebink, J. Kennedy, M. Romansky, “Manufacturing and Reliability Screening of Lower Melting Point, Pb-Free Alloys Containing Bismuth”, Journal of Microelectronics and Electronic Packaging, Volume 12, Number 1, pp. 1-28, First Quarter 2015.
5. S. Shirazi, L. Yin, S. Khasawnch, L. Wentlent, P. Borgesen, “Effects of Solder Joint Dimensions and Assembly Process on Acceleration Factors and Life in Thermal Cycling of SnAgCu Solder Joints”, IEEE 2015 Electronics Components & Technology Conference.
6. IPC-9701A, Performance Test Methods and Qualification Requirements for Surface Mount Solder Attachments, www.ipc.org, February 2006.

**APPENDIX A**

**General Factorial Regression: Cycles versus Test_Temp, SF, Tech**

**Factor Information**

| Factor | Levels | Values |
|---|---|---|
| Test_Temp | 4 | -55, 25, 75, 125 |
| SF | 2 | ENIG, OSP |
| Tech | 2 | BGA_1, PLCC |

**Analysis of Variance**

| Source | DF | Adj SS | Adj MS | F-Value | P-Value |
|---|---|---|---|---|---|
| Model | 12 | 8.25582E+11 | 68798509912 | 12.49 | 0.000 |
| Linear | 5 | 5.97179E+11 | 1.19436E+11 | 21.68 | 0.000 |
| Test_Temp | 3 | 5.50499E+11 | 1.83500E+11 | 33.31 | 0.000 |
| SF | 1 | 4482528868 | 4482528868 | 0.81 | 0.380 |
| Tech | 1 | 38874525400 | 38874525400 | 7.06 | 0.017 |
| 2-Way Interactions | 7 | 2.13756E+11 | 30536611649 | 5.54 | 0.002 |
| Test_Temp*SF | 3 | 1.53214E+11 | 51071415073 | 9.27 | 0.001 |
| Test_Temp*Tech | 3 | 54101847380 | 18033949127 | 3.27 | 0.047 |
| SF*Tech | 1 | 13779965 | 13779965 | 0.00 | 0.961 |
| Error | 17 | 93636929068 | 5508054651 | | |
| Lack-of-Fit | 2 | 23688863365 | 11844431683 | 2.54 | 0.112 |
| Pure Error | 15 | 69948065702 | 4663204380 | | |
| Total | 29 | 9.19219E+11 | | | |

**Model Summary**

| S | R-sq | R-sq(adj) | R-sq(pred) |
|---|---|---|---|
| 74216.3 | 89.81% | 82.62% | 69.73% |

**Coefficients**

| Term | Coef | SE Coef | T-Value | P-Value | VIF |
|---|---|---|---|---|---|
| Constant | 273706 | 15149 | 18.07 | 0.000 | |
| Test_Temp | | | | | |
| -55 | 231264 | 23953 | 9.65 | 0.000 | 1.67 |
| 25 | -68303 | 32137 | -2.13 | 0.049 | 2.60 |
| 75 | -65731 | 23953 | -2.74 | 0.014 | 1.67 |
| SF | | | | | |
| ENIG | 13666 | 15149 | 0.90 | 0.380 | 1.24 |
| Tech | | | | | |
| BGA_1 | -40246 | 15149 | -2.66 | 0.017 | 1.24 |
| Test_Temp*SF | | | | | |
| -55 ENIG | 104280 | 23953 | 4.35 | 0.000 | 1.67 |
| 25 ENIG | 22280 | 32137 | 0.69 | 0.497 | 2.60 |
| 75 ENIG | -70471 | 23953 | -2.94 | 0.009 | 1.67 |
| Test_Temp*Tech | | | | | |
| -55 BGA_1 | -55665 | 23953 | -2.32 | 0.033 | 1.67 |
| 25 BGA_1 | -26930 | 32137 | -0.84 | 0.414 | 2.60 |
| 75 BGA_1 | 38920 | 23953 | 1.62 | 0.123 | 1.67 |
| SF*Tech | | | | | |
| ENIG BGA_1 | -758 | 15149 | -0.05 | 0.961 | 1.24 |